

CHEMISTRY

A European Journal

A Journal of



Accepted Article

Title: Title Synthesis of α -L-fucopyranoside-presenting glycoclusters and investigation of their interaction with recombinant Photorhabdus asymbiotica lectin (PHL)

Authors: Jančaříková Gita, Mihály Herczeg, Eva Fajdiarová, Josef Houser, Katalin E. Kövér, Anikó Borbás, Michaela Wimmerová, and Magdolna Csávás

This manuscript has been accepted after peer review and appears as an Accepted Article online prior to editing, proofing, and formal publication of the final Version of Record (VoR). This work is currently citable by using the Digital Object Identifier (DOI) given below. The VoR will be published online in Early View as soon as possible and may be different to this Accepted Article as a result of editing. Readers should obtain the VoR from the journal website shown below when it is published to ensure accuracy of information. The authors are responsible for the content of this Accepted Article.

To be cited as: *Chem. Eur. J.* 10.1002/chem.201705853

Link to VoR: <http://dx.doi.org/10.1002/chem.201705853>

Supported by
ACES

WILEY-VCH

Synthesis of α -L-fucopyranoside-presenting glycoclusters and investigation of their interaction with *Photorhabdus asymbiotica* lectin (PHL)

Gita Jančaříková,^[a,b] Mihály Herczeg,^[c] Eva Fudiarová,^[b] Josef Houser,^[a,b] Katalin E. Kövér,^[d] Anikó Borbás,^{*[c]} Michaela Wimmerová^{*[a,b,e]} and Magdolna Csávás^{*[c]}

Dedicated to Professor Pál Herczegh on the occasion of his 70th birthday.

Abstract: *Photorhabdus asymbiotica* is a gram-negative bacterium that is not only as effective an insect pathogen as other members of the genus, but it also causes serious diseases in humans. The recently identified lectin PHL from *P. asymbiotica* verifiably modulates an immune response of humans and insects, which supports the idea that the lectin might play an important role in the host-pathogen interaction. Dimeric PHL contains up to seven L-fucose specific binding sites per monomer, and in order to target multiple binding sites of PHL, α -L-fucoside-containing di-, tri- and tetravalent glycoclusters were synthesized. Methyl gallate and pentaerythritol were chosen as multivalent scaffolds, and the fucoclusters were built from the above-mentioned cores by coupling with different oligoethylene bridges and propargyl α -L-fucosides using 1,3-dipolar azide-alkyne cycloaddition. The interaction between fucoside derivatives and PHL was investigated by several biophysical and biological methods, ITC and SPR measurements, hemagglutination inhibition assay and an investigation of bacterial aggregation properties were carried out. Moreover, details of the interaction between PHL and propargyl α -L-fucoside as a monomer unit were revealed using X-ray crystallography. Besides this, the interaction with multivalent compounds was studied by NMR techniques. The newly synthesized multivalent fucoclusters proved to be up to several orders of magnitude better ligands than the

natural ligand, L-fucose.

Introduction

Photorhabdus asymbiotica together with another three species (*P. luminescens*, *P. temperata* and *P. heterorhabditis*) belongs to the *Photorhabdus* genus – entomopathogenic bacteria forming a symbiotic relationship with nematodes from the genus *Heterorhabditis*. Unlike other *Photorhabdus* species, *P. asymbiotica* is unique in its ability to act as an emerging human pathogen. It causes invasive soft tissue infections that are difficult to treat locally, and disseminated bacteraemic disease characterized by multifocal skin and soft tissue abscesses.^[1–4] Analysis of the *P. asymbiotica* genome identified the fucose/galactose-binding lectin PHL.^[5] It was revealed that PHL has the ability to act as a host-cell recognizing agent through interacting with the haemolymph of *Galleria mellonella* (order Lepidoptera, family Pyralidae) and human blood components. Therefore, PHL could be considered to be a usable therapeutic target.

The soluble lectin PHL forms a seven-bladed β -propeller assembling into a homo-dimer with an inter-subunit disulphide bridge. The crystal structure of the complex with different ligands demonstrated the existence of two sets of binding sites per monomer with preferences for L-fucose and D-galactose, respectively. Biophysical studies show an affinity of PHL mainly for α -L-fucosides over other tested ligands. Recent analysis of PHL/Me- α -L-Fuc complexes revealed up to seven potential fucose-binding sites per PHL monomer, forming a circle.^[5] On the basis of biological tests, a specific agglutination of type O human red blood cells (RBCs) was observed as well as interaction with all types of RBCs through α -fucoside. These outcomes suggest that this lectin could be also directly involved in the adhesion to host cells. This leads to the need for glyco-inhibitors which can strongly bind to the lectin to compete with and disrupt host-lectin interaction during the first step of the infection process.

PHL as a multivalent lectin displays an avidity effect, which significantly increases affinity towards its ligands. For that reason, compounds containing multiple carbohydrate moieties could be the most potent inhibitors. A new set of tri- and tetravalent glycoclusters with different architectures and valences were designed to provide an opportunity to evaluate the impact of topology and valency on binding properties toward PHL. Here, we present the preparation of di-, tri- and tetravalent

[a] G. Jančaříková, Dr. J. Houser, Prof. M. Wimmerová
Central European Institute of Technology
Masaryk University
Kamenice 5, 625 00 Brno, Czech Republic
E-mail: michaw@chemi.muni.cz

[b] G. Jančaříková, E. Fudiarová, Dr. J. Houser, Prof. M. Wimmerová
National Centre for Biomolecular Research, Faculty of Science
Masaryk University
Kotlářská 2, 611 37 Brno, Czech Republic

[c] Dr. M. Herczeg, Prof. A. Borbás, Dr. M. Csávás
Department of Pharmaceutical Chemistry
University of Debrecen
Egyetem tér 1, H-4032, Debrecen, Hungary
E-mail: borbas.aniko@pharm.unideb.hu,
csavas.magdolna@science.unideb.hu

[d] Prof. K. E. Kövér
Department of Inorganic and Analytical Chemistry
University of Debrecen
Egyetem tér 1, H-4032, Debrecen, Hungary

[e] Prof. M. Wimmerová
Department of Biochemistry, Faculty of Science
Masaryk University
Kamenice 5, 625 00 Brno, Czech Republic

Supporting information for this article is given via a link at the end of the document.

fucoclusters and study their interaction with the recombinant PHL lectin from *P. asymbiotica*.

Results and Discussion

Synthesis

Similarly to our recent works^[6,7], propargylated methyl gallate **1**^[8] and pentaerythritol **2**^[9] were chosen as multivalent scaffolds, and heterobifunctionalized tetraethylene glycol **3**^[10] and ethylene glycol **4**^[11] were used as linkers with different lengths. Based on the known X-ray structure of PHL, the average distances between the fucose-binding sites is approximately 19 Å, so these linkers are long enough that the α -L-fucose-units of the fucoclusters are able to bind to more than one binding pocket of the lectin.

We efficiently prepared propargyl α -L-fucoside **5** by Fischer glycosylation using sulfamic acid^[12] and utilized it in both unprotected and acetylated form **6**^[13] to create multivalent structures (Figure 1).

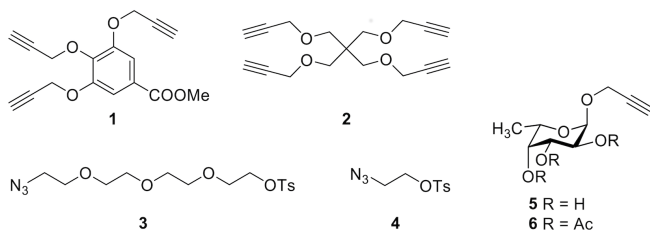


Figure 1. Building blocks for the fucoclusters.

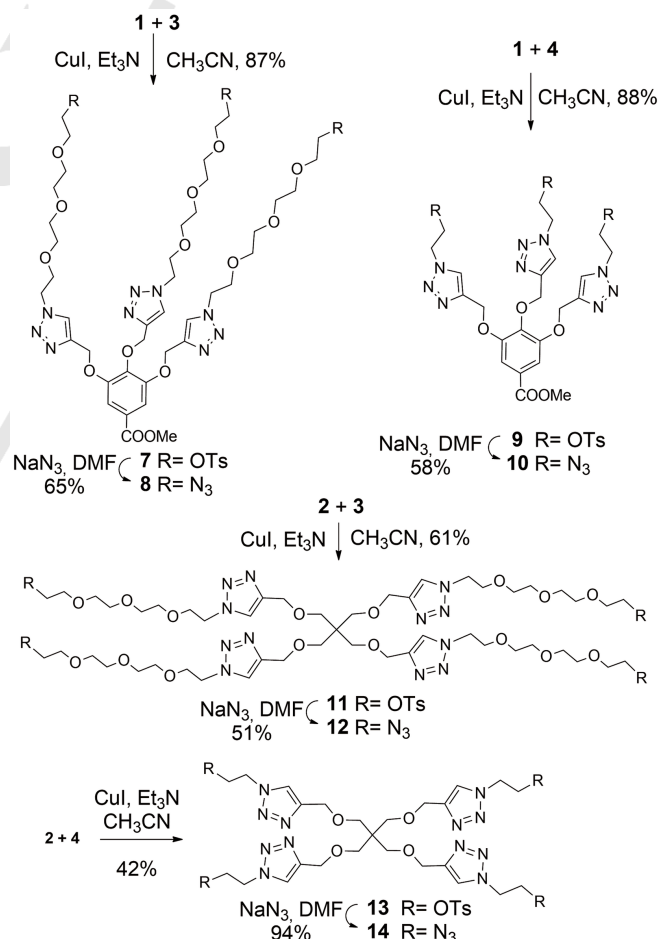
The fucoclusters were built from the above structural elements from the inside out starting from the central cores applying two consecutive 1,3-dipolar azide-alkyne cycloaddition click reactions. First, the tri- and tetravalent cores **1** and **2** were coupled with bridges **3** and **4**, respectively, via the copper(I)-catalyzed azide-alkyne cycloaddition click reaction (CuAAC) to obtain tosylated compounds **7**, **9**, **11** and **13**, in good yields. The tosyl groups of all scaffolds were converted into azido functional groups using sodium azide to result in compounds **8**, **10**, **12** and **14**, which were also suitable for further click reactions (Scheme 1).

Scaffolds containing tetraethylene glycol bridges **8** and **12** were coupled by CuAAC reaction with propargyl 2,3,4-tri-O-acetyl- α -L-fucopyranoside **6** to produce the protected fucoclusters **15** and **17**, respectively, while click reaction between the same scaffolds and propargyl α -L-fucopyranoside **5** provided the final products **16** and **18** directly (Scheme 2). The latter two compounds were also obtained by the Zemplén deacetylation of **15** and **17**, respectively. Comparing the above syntheses with the unprotected and protected sugars **5** and **6**, using the free fucose was not only a shorter, but also a more efficient procedure, although the isolation and purification were more demanding. (While the overall yields of compounds **16** and **18** were 60% and 65% respectively using free fucoside, these yields decreased to 38% and 32% when using the protected fucoside.) For this

reason, we chose the shorter reaction pathway for further synthesis.

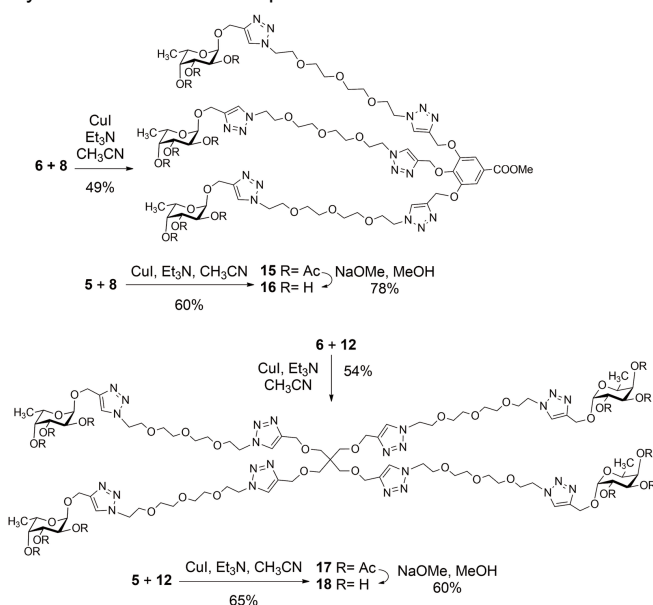
Based on the same strategy, scaffolds **10** and **14** equipped with an ethylene glycol bridge were reacted with propargyl α -L-fucopyranoside **5** by copper(I)-catalyzed cycloaddition to result in the final products **19** and **20** (Scheme 3).

Our further aim was the examination of the role and effect of the linker and the triazole-ring in the lectin-carbohydrate interactions. For this reason, compounds **5**, **22** and **23** were also provided for biological investigations. Compound **5** (propargyl α -L-fucoside) is suitable for investigations to define the role of the monomer L-fucose. Moreover, compound **5** was reacted with azido-tetraethylene glycol derivative **4** under the condition of click reaction, then tosyl group was subsequently replaced with azide, to yield compound **22** (49% for two steps), which can provide information about the potency of the ethylene glycol linker-armed monomer. Finally, compound **5** was coupled with diazido-tetraethylene glycol **21**^[14] via click reaction, to yield compounds **23** (35%) and **24** (12%), which can serve information about the binding properties of the tetraethylene glycol linker-armed monomer and dimer (Scheme 4).

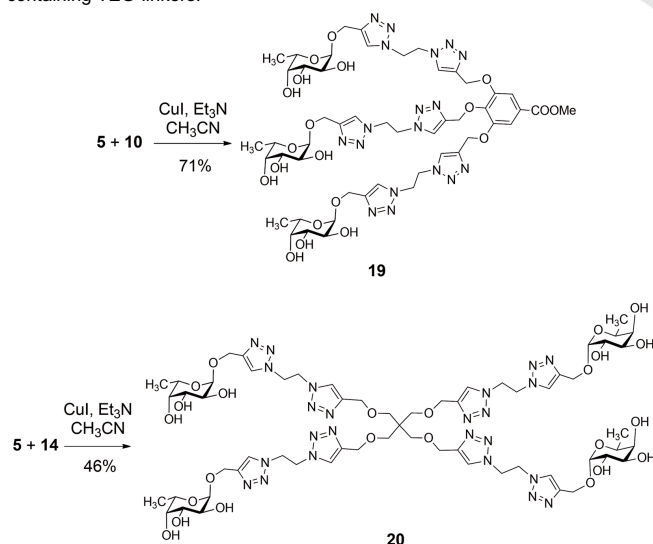


Scheme 1. Synthesis of multivalent scaffolds having functionalized ethylene glycol (**10** and **14**) and tetraethylene glycol (**8** and **12**) linker arms.

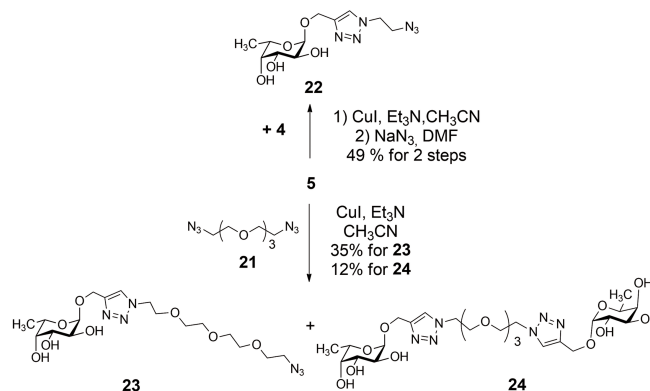
The interaction of mono- and multivalent fucosylated ligands with PHL was investigated by a few methods. At first hemagglutination inhibition assay was utilized as a simple microscopy method to preselect the most efficacious inhibitors. Subsequently two biophysical techniques - isothermal titration calorimetry (ITC) and surface plasmon resonance (SPR) - were employed. The presence of fucose-binding lectins on the surface of *P. asymbiotica* subsp. *australis* was indirectly tested through the cross-linking of bacterial cells caused by multivalent ligands. In summary, these methods provide information about the binding affinity, inhibition potency and effect of the compounds on cell cross-linking. For a better structural characterization of the interaction of PHL with ligands, ligand-soaking of PHL crystals and STD-NMR experiments were carried out.



Scheme 2. Synthesis of tri- and tetravalent fucodendrons **16** and **18** containing TEG-linkers.



Scheme 3. Synthesis of tri- and tetravalent α -L-fucoside-containing dendrons **19** and **20** having short linker arms.



Scheme 4. Synthesis of the linker-armed monomers **22** and **23**.

Hemagglutination inhibition assay

PHL, being a fucose-specific lectin, was shown to agglutinate papain-treated RBCs of blood group O^[5] with surface-exposed terminal trisaccharide α -L-Fucp-(1 \rightarrow 2)- β -D-Galp-(1 \rightarrow 3/4)-D-GlcpNAc. This property was also used to assess the inhibition potency of the set of α -L-fucoside molecules on hemagglutination by PHL (Figure 2). All of them were able to inhibit the hemagglutination with at least four times higher potency than L-fucose (Table 1). Tetravalent compound **18** was shown to be the most efficient inhibitor followed by compounds **16**, **19** and **20**, all of them being half as efficient as **18**. Compound **20** is also a tetravalent fucocluster, but contains shorter linkers, which may be not able to connect binding sites, in contrast to compound **18**.

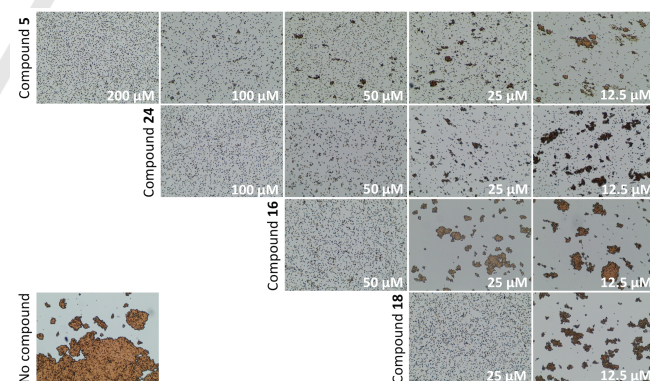


Figure 2. Representatives of mono-, di-, tri-, and tetra-fucosylated compounds and their influence on hemagglutination of RBC O caused by PHL. Two-fold serially diluted carbohydrate compounds **5**, **24**, **16** and **18** were able to inhibit hemagglutination at minimal concentrations 200 μ M, 100 μ M, 50 μ M and 25 μ M, respectively. Hemagglutination of RBC O caused by PHL without inhibitor is shown on the picture in the left down corner.

Table 1. Hemagglutination inhibition assay with PHL. Minimal inhibitory concentrations (MIC) of synthesized inhibitors and their potency towards L-fucose was determined. To assess the contribution of valency to the MIC, an affinity improvement factor β was calculated as the relationship $MIC_{L-fucose}/(valency \times MIC_{ligand})$.

Ligand	Valency	MIC [μ M]	Potency	β
L-Fuc	1	3,200	1	1
Compound 23	1	800	4	4
Me- α -L-Fuc	1	400	8	8
Compound 5	1	200	16	16
Compound 22	1	200	16	16
Compound 24	2	100	32	16
Compound 19	3	50	64	21
Compound 16	3	50	64	21
Compound 20	4	50	64	16
Compound 18	4	25	128	32

Surface plasmon resonance

The surface plasmon resonance (SPR) technique was employed to analyse the competitive inhibition of PHL binding to a multivalent chip surface. The experiments were performed using a constant concentration of PHL and increasing concentration of the studied compounds to enable the determination of IC_{50} . Tetravalent compounds **18** and **20** appeared to be the most efficient inhibitors, with IC_{50} reaching 200 nM and 96 nM, respectively (Table 2). The trivalent compounds **16** and **19** had a weaker inhibitory potential, but were still in the nanomolar range, which is three orders of magnitude lower than for free L-fucose. The monovalent ligands proved to be at least three times more efficient than L-fucose. Logarithmic plots of IC_{50} and the inhibition curves from SPR measurements displayed in Figure 3 nicely demonstrate the growing inhibitory effect through monovalent, divalent and tri-/tetravalent α -L-fucoside compounds.

Table 2. Inhibitory effect of representative carbohydrates on PHL binding to immobilized L-fucoside. IC_{50} was determined from a plot of serial dilutions vs. % inhibition, and potency was relative to L-Fuc. To assess the contribution of valency to the IC_{50} , an affinity improvement factor β was calculated as the relationship $IC_{50,L-fucose}/(valency \times IC_{50,ligand})$.

Ligand	Valency	IC_{50} [μ M]	Potency	β
L-Fuc	1	361	1	1
Compound 23	1	108	3	3
Me- α -L-Fuc	1	68	5	5

Compound 5	1	54	7	7
Compound 22	1	52	7	7
Compound 24	2	3.2	118	59
Compound 19	3	0.37	979	326
Compound 16	3	0.35	1030	343
Compound 20	4	0.20	1806	452
Compound 18	4	0.10	3784	946

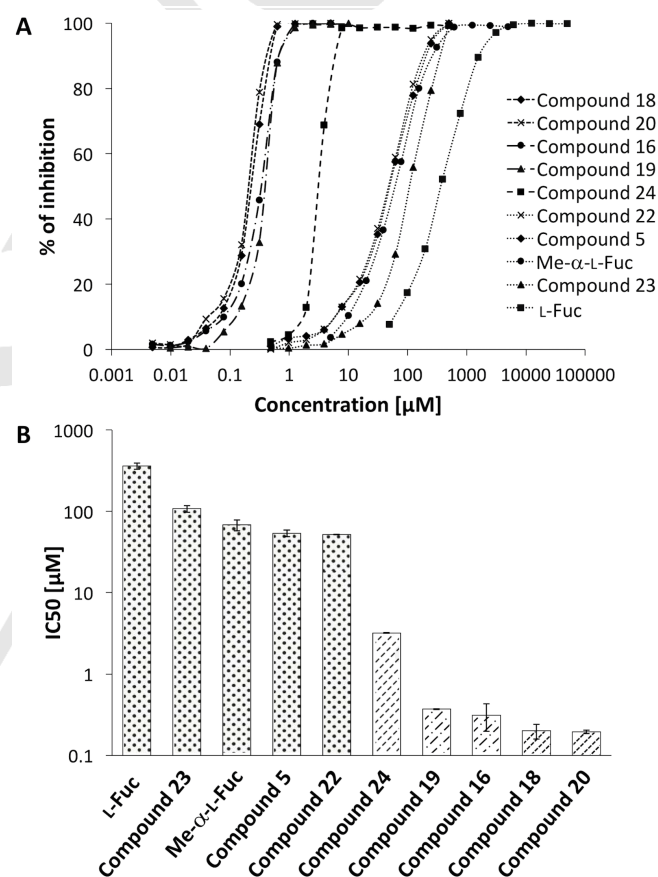


Figure 3. IC_{50} determination of fucoclusters towards PHL from SPR measurements. (A) A logarithmic plot of inhibition curves determined from SPR experiments. Individual types of line correspond to monovalent (dotted), divalent (dashed), trivalent (dashdotted) and tetravalent (densely dashed) ligands. (B) A logarithmic plot of IC_{50} for individual mono-/multivalent α -L-fucoside compounds. Standard deviations were calculated from three independent measurements. Individual type of pattern corresponds to monovalent (dotted), divalent (dashed), trivalent (dashdotted) and tetravalent (densely dashed) ligands.

Isothermal titration calorimetry

The binding of PHL to multivalent α -L-fucoside compounds was further characterized by isothermal titration calorimetry (ITC) to

determine the complete thermodynamic profile of the molecular interactions. As for monovalent fucoclusters, all of them were proved to be low-affinity ligands for PHL. The data for compound **23** were impossible to evaluate. The other two monovalent ligands provided better results. In both cases, the ITC curves indicated a low affinity toward PHL, as usually observed for lectin/saccharide interactions (Figure 4). The stoichiometry value n was assessed to be around 4 and the dissociation constants were in the submillimolar range (Table 3). As expected, the enthalpy of binding for shorter compounds was less negative than for longer chains. Shorter and more rigid compounds **5** and **22** also exhibited a positive entropy contribution, in contrast to other studied molecules.

The ITC data for multivalent fucosylated compounds provided a more interesting set of results (Table 3 and Figure 4). The values indicate a strong interaction between PHL and multivalent fucoclusters, with an affinity in the low micromolar range. The stoichiometry varies between 2 and 3 ligand molecules per PHL monomer. Generally, tetravalent ligands exhibited a higher affinity than tri- or divalent ones, however, an

interesting effect of linker length was observed. Short linkers seem to disfavour ligand binding. Thus, compounds with shorter linkages (tetravalent **20** and trivalent **19**) bind with considerably lower affinity than longer linker-containing tetravalent **18** and trivalent **16**, respectively. Unusually high enthalpy and entropy contributions were observed for compound **19**. This suggests the possibility of a different binding mode being employed.

The highest affinity was observed towards tetravalent compound **18**, with a K_D twice as good as the second best tetravalent compound **20**, and more than a thousand times better than free L-Fuc. It is interesting that trivalent compound **16** containing longer linkers has a comparable K_D to tetra-fucosylated compound **20** with a shorter spacer – the spacer length plays an important role in affinity. Likewise, dimeric fucocluster **24** is a little bit better than trivalent compound **19** with short linkers (Figure 4B).

During the ITC measurements, we also observed an additional effect – the cross-linking of PHL caused by multivalent fucoclusters that was accompanied by the formation of visible precipitates.

Table 3. Thermodynamic profiles for interaction between PHL and carbohydrate ligands determined by isothermal titration calorimetry using one site model fitting procedure at 25 °C (standard deviations were calculated from two independent measurements). To assess the contribution of valency to the affinity increase, an affinity improvement factor β was calculated as the relationship $K_{D,L-fucose}/(\text{valency} \times K_{D,\text{ligand}})$.

Ligand	Valency	n	K_D [μM]	ΔH [kJ mol^{-1}]	$-\Delta S$ [kJ mol^{-1}]	ΔG [kJ mol^{-1}]	β
Compound 23	1	ND ^[a]	ND ^[a]	ND ^[a]	ND ^[a]	ND ^[a]	ND ^[a]
L-Fuc	1	3 ^[b]	1,395 ± 34	-59.5 ± 1.0	43.2	-16.3 ± 0.3	1
Me- α -L-Fuc	1	2.9 ± 0.2	267 ± 11	-59.0 ± 4.2	38.6	-20.4 ± 1.5	5
Compound 22	1	4.0 ± 0.3	175 ± 18	-14.6 ± 1.4	-6.9	-21.5 ± 2.1	8
Compound 5	1	4.6 ± 0.3	149 ± 16	-8.8 ± 0.7	-13.1	-21.9 ± 1.8	9
Compound 19	3	2.3 ± 0.0	8.5 ± 0.5	-65.4 ± 0.7	36.5	-28.9 ± 0.3	55
Compound 24	2	2.5 ± 0.0	6.6 ± 0.7	-42.2 ± 0.8	12.5	-29.7 ± 0.6	106
Compound 16	3	2.9 ± 0.1	3.6 ± 0.8	-54.4 ± 1.4	23.4	-31.0 ± 0.8	129
Compound 20	4	2.1 ± 0.1	3.1 ± 1.0	-56.9 ± 2.3	25.5	-31.4 ± 1.2	113
Compound 18	4	1.9 ± 0.0	1.2 ± 0.4	-77.5 ± 2.6	43.6	-33.9 ± 1.1	290

[a] Values not determined because of low affinity interaction. One-site model for compound **23** was unable to reach a meaningful fit. [b] The stoichiometry value of L-fucose was fixed during fitting procedure because of low-affinity interaction. The value was derived from the X-ray crystal structure of the PHL/Me- α -L-Fuc complex.

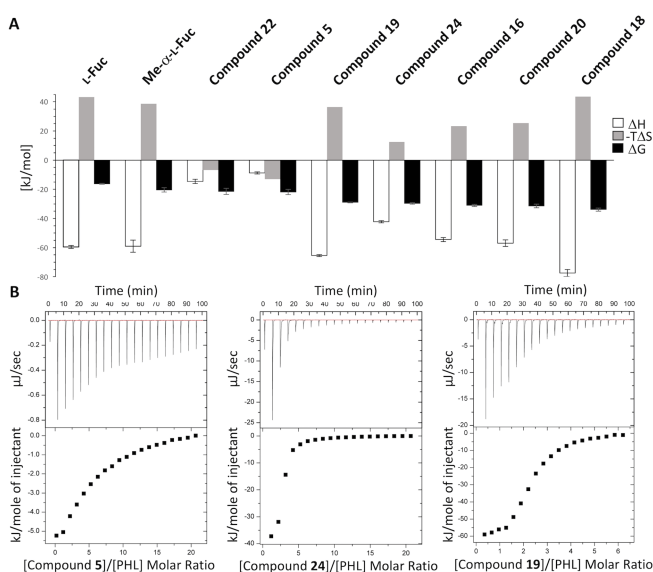


Figure 4. (A) Thermodynamic profiles for interaction between PHL and mono/multivalent α -L-fucoside compounds determined by isothermal titration calorimetry at 25 °C (standard deviations were calculated from two independent measurements). (B) Selected ITC curves of PHL (50 μ M) titration by compound **5** (5 mM), **24** (5 mM) and **19** (1.5 mM). 20 injections of 2.0 μ l of fucoclusters were added every 240 s to a PHL-containing cell. Lower plots show the total heat released as a function of total ligand concentration for the titration shown in the upper panels.

Aggregation of PHL lectin monitored by ^1H NMR spectroscopy

The aggregation behaviour of the PHL lectin upon titration with the five α -L-fucoside-containing derivatives (monomer **5**, trivalent **16** and **19** and tetravalent **18** and **20**) has been subsequently investigated and compared by ^1H NMR spectroscopy, monitoring the change (decrease) in protein signal intensity as a function of the actual ligand concentration (Figure 5). For a fair comparison of the extent of PHL aggregation, each tested fucoside ligand was added to a similar (ca. 40–50 μ M) solution of PHL in concentrations ranging from 6 to 25 μ M. Before each titration assay, a regular ^1H NMR spectrum was recorded on the sample containing PHL alone, providing the reference protein signal intensity for quantification of protein aggregation during the subsequent titration steps. As expected, the monovalent ligand **5** did not lead to any noticeable aggregation of PHL, even when its concentration was increased up to 0.1 mM. In contrast, when titrating the multivalent ligands into the sample containing PHL a significant reduction (drop) in the protein signal envelope was observed, suggesting the formation of large, non-soluble aggregates via possible cross-linking between the multivalent ligands and PHL. The level of aggregation, however, varied

according to the type and concentration of the multivalent ligand tested. The tri- and tetravalent fucodendron derivatives containing TEG-linkers (**16** and **18**, respectively) led to the formation of smaller amount of non-soluble aggregates than the ones (**19**, **20**) with the shorter linker arm. Specifically, at 6.2 μ M of fucodendrons with a TEG-linker, about 30 % of total protein aggregated (precipitated), while upon adding the ligands with a shorter linker at the same concentration, only ca. 50 % of the protein remained in solution.

X-ray structure of PHL/compound 5 complex

The PHL lectin was shown to form a dimeric structure consisting of two seven-bladed β -propellers with two types of binding sites situated between the blades.^[5] Both types of binding sites have different amino acid composition and binding preferences. Also, the non-identity of individual potential binding sites within the same type was proposed. The direct study of complexes with branched fucosylated structures was not possible, as mixing PHL with the multivalent compound leads to protein precipitation, preventing the co-crystallization. Soaking ligand-free PHL crystals with a low concentration of individual branched compounds did not result in complex formation, while soaking with their higher concentrations led to a crystal decomposition. Therefore, to determine the potential PHL binding sites for studied molecules, we soaked the crystals with monomeric compound **5**.

The structure of the PHL/compound **5** complex was determined using X-ray diffraction (Table 4). The lectin in the complex retains the seven-bladed β -propeller fold (Figure 6A, B) identical to the ligand-free form.^[6] The differential electron density map was clear enough to identify compound **5** monomers in five of the seven potential fucose binding sites of monomer A – site 1F, 3F, 5F, 6F and 7F (Figure 6C). In monomer B, the ligand binding in site 5F was affected by intermonomeric contacts in the crystal, and it was not possible to determine the precise position of the ligand. Compound **5** is bound via its fucosylated part, which adopts the same orientation as Me- α -L-Fuc in the previously determined PHL/Me- α -L-Fuc complex.^[5] Thus, the O3, O4 and O5 of the fucosyl part is coordinated to the protein backbone of the Gly/Gln and Val residues on one side of the pocket and backbone and side chain of the Thr residue on the other side of the pocket. The C6 methyl group and hydrophobic surface of Fuc C3, C4 and C5 are stabilized through CH- π interactions with two Trp residues, and O3 may be further stabilized by a water bridge to the neighbouring Asp residue (Figure 6C – sites 3F, 5F, 7F). Compared to the PHL/Me- α -L-Fuc complex, more binding sites were occupied by compound **5**, which agrees with the higher affinity towards compound **5** than towards Me- α -L-Fuc, as was determined by ITC and hemagglutination inhibition experiments.

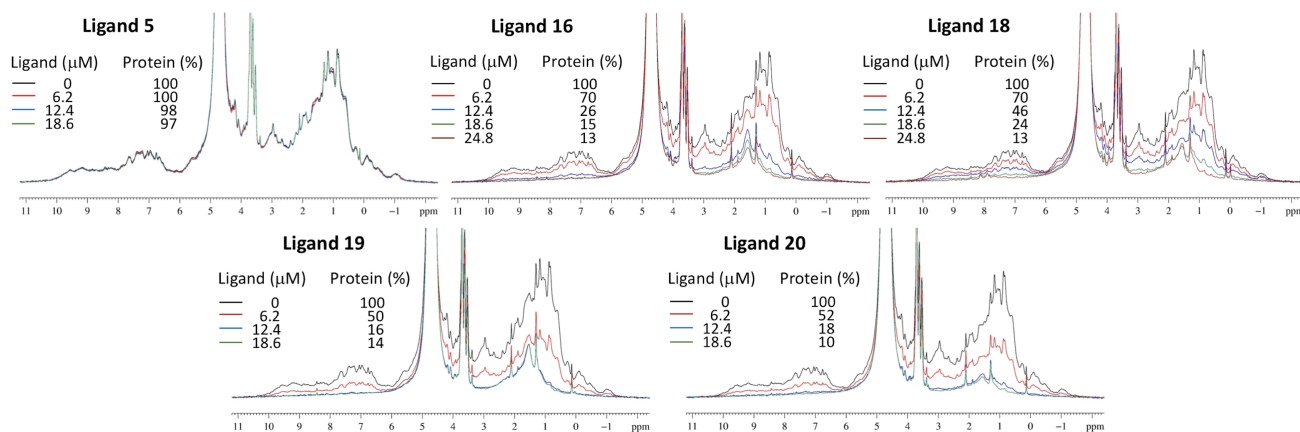


Figure 5. ^1H NMR experiments (500 MHz, $T = 298$ K) for monitoring the aggregation of the PHL lectin in the presence of increasing concentration of the ligands (**5**, **16**, **18**, **19** and **20**). 40–50 μM solution of PHL in D_2O (PBS) was titrated by increasing amount of ligands. The relevant ligand concentrations together with the percentage of PHL remaining in solution (referenced to pure PHL solution) are given above the spectra. All NMR spectra were recorded with 512 number of scans, allowing 1 s for relaxation between subsequent transients.

Table 4. Data-collection and refinement statistics for PHL/compound **5** complex. Values in parentheses correspond to the highest resolution shell.

PDB ID	6F5W
Beamline	BESSY, 14.1
Wavelength (Å)	0.9184
Space group	P3 ₂ 21
Unit-cell parameters	
a and b (Å)	80.57
c (Å)	224.80
Resolution range (Å)	44.96–1.91 (1.96–1.91)
Reflections measured	733262 (97948)
Unique reflections	66991 (9584)
Completeness (%)	99.8 (98.26)
CC1/2	99.6 (66.2)
R_{merge}	0.206 (1.319)
Multiplicity	10.9 (10.2)
$\langle I/\sigma(I) \rangle$	9.4 (1.8)
Reflections used	63648
Reflections used for R_{free}	3273
R factor (%)	17.28
R_{free} (%)	21.28
R.m.s.d. bond lengths (Å)	0.011
R.m.s.d. bond angles (°)	1.43
No. of water molecules	465

No. of non-H atoms (total)	5991
Ramachandran plot	
Residues in most favorable regions (%)	96.9
Residues in allowed regions (%)	3.1

Unexpectedly, the clear electron density for compound **5** was also identified in the galactose-binding site 4G (Figure 6D). The ligand is coordinated by the same residues as in the case of D-Gal, however the orientation is different, with the aliphatic chain on O1 pointing outwards. The ligand is bound via a hydrogen bond network to the side chains of Arg186 (O1 and O2), Glu188 and Gln251 (O2 and O3), Trp259 (O3 and O4) and backbone of Gly257 (O4). The ligand is further stabilized by a water bridge between Glu215 and O4, a CH- π interaction with Trp202 and cation- π interaction between the guanidinium group of Arg186 and propargyl group of the ligand. Based on this observation, we can propose the possible design of a single inhibitor that would target both types of PHL binding sites at the same time.

Binding of fucoside-containing ligands to PHL lectin characterized by ^1H STD and competition STD NMR experiments

STD NMR experiments^[15–17] were performed to support and further characterize the binding of α -L-fucoside-containing ligands to PHL. The corresponding spectra are in Figure 7. For the monovalent ligand **5**, clear STD effects were observed for all sugar ring protons. The percentage STD intensities were similar for protons H1–H4 (~100 %), while H5 and the CH₃ protons exhibited slightly smaller STD effects (55 % and 82 %, respectively). These facts indicate the direct involvement of the sugar ring in the binding to the lectin. A significant STD response (74 %) was also observed for the CH₂ protons of the propargyl group, suggesting that the binding event may involve

this group as well. It should be noted, however, that the intensity of the propargyl CH-proton is significantly reduced due to partial deuteration in D₂O, therefore its STD response is likely also attenuated and so that not quantified in %. It should be also mentioned that the irradiation of the protein in the aromatic signal region led to a significantly lower saturation of all ligand protons with correspondingly smaller STD effects. This fact may suggest that the binding pocket of the PHL lectin probably involves more aliphatic than aromatic amino acid residues responsible for sugar binding.

To monitor the binding of the high-affinity multivalent ligands and to identify their probable binding sites, competition STD

experiments were also carried out. The corresponding STD spectra are shown in Figure 7B. As can be seen, all STD signals decreased considerably upon adding the multivalent ligands (first trivalent, **16**, lastly tetravalent, **18**) to the sample initially containing the monovalent ligand alone. These data may confirm that both multivalent ligands compete with the monovalent ligand for the same or at least partially the same (overlapping) binding site of the PHL lectin.

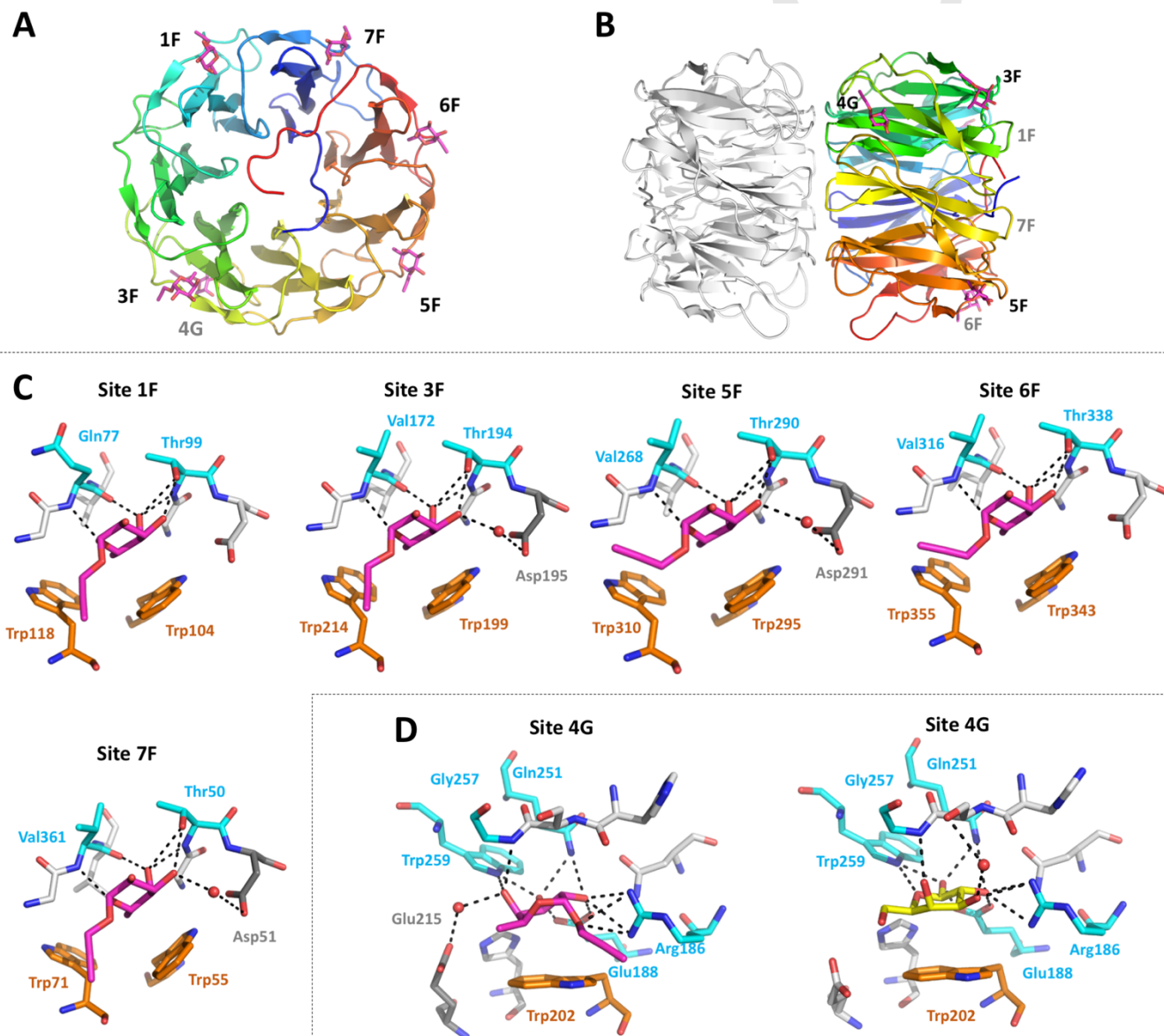


Figure 6. Structure of PHL complex with compound 5. (A) PHL monomer (chain A) overall architecture with compound **5** shown as magenta sticks. Individual binding sites are labelled in black (front plane) or grey (back plane) (B) Side view of PHL dimer with chain B shown in grey and without ligands. (C) Individual PHL fucose-type binding sites with compound **5** (magenta) bound. Amino acids responsible in ligand binding are highlighted and labelled. (D) PHL galactose-type binding site with compound **5** (magenta) bound and PHL galactose-type binding site with D-Gal (yellow) bound (PDB ID: 5MXH). Colour code for panels C/D: amino acids involved in ligand-binding through H-bond – cyan, CH- π interaction – orange or water bridge – grey.

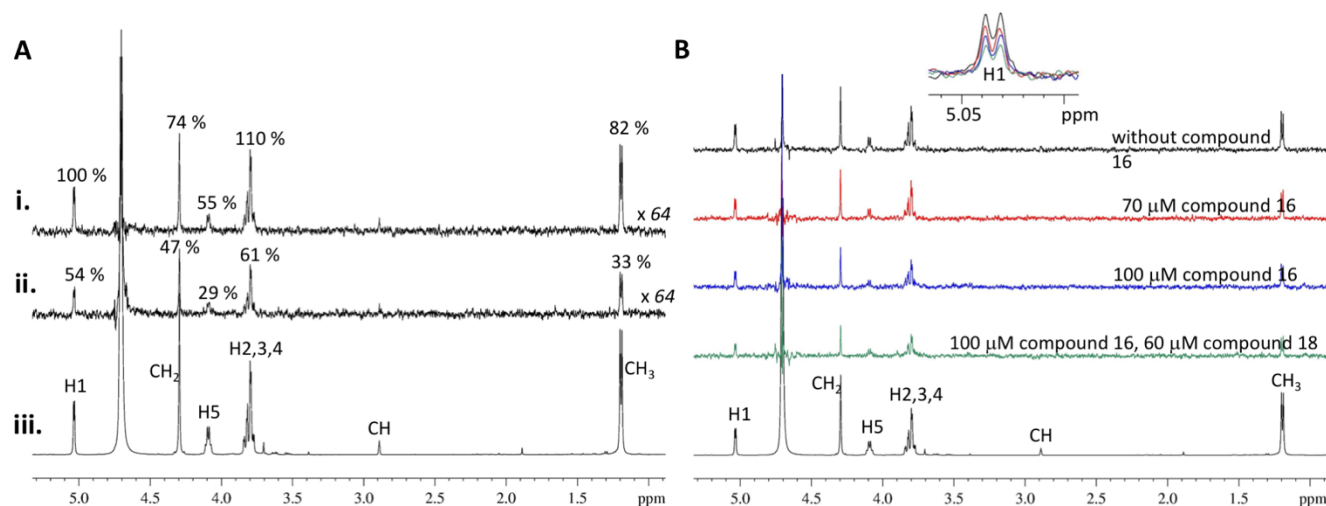


Figure 7. (A) STD experiments for the monovalent fucoside ligand **5** complexed with the PHL lectin. The estimated molar ratio of sugar/lectin is ca. 100/1. i.-ii.) The corresponding STD spectra (up-scaled by a factor of 64) depicted after saturating for 3 s at δ -1.5 and 10.5 ppm, respectively. The percentage STD intensities are referenced to the STD response of H-1 proton (100 %) obtained upon irradiation at the aliphatic signal region of PHL at -1.5 ppm. On- and off-resonance data were acquired alternately up to total of 1424 scans recorded for each FID; iii.) The regular 500 MHz 1D ¹H NMR spectrum with the assignment of resonances. (B) Competition STD experiments for characterizing the binding of the high affinity ligands (**16** and **18**) to PHL. The bottom spectrum corresponds to the regular ¹H NMR spectrum of ligand **5**. The other spectra are the corresponding STD responses recorded on samples containing the ligand **5** at constant 2 mM concentration, while the multivalent ligands were subsequently added in increasing concentrations. The top (reference) STD spectrum corresponds to the sample containing only the monovalent ligand. The other spectra were recorded on samples containing trivalent ligand **16** at 70 μM; at 100 μM; and lastly, the mixture of trivalent **16** at 100 μM and tetravalent **18** at 60 μM. For better visualization of the STD signal drop due to competition, an overlay of the STD responses of H1 is shown in the inset at larger scale. Note that during titration no aggregation of protein was observed.

***P. asymbiotica* cross-linking - Bacterial aggregation properties**

The aggregation of PHL by multivalent fucoclusters was observed in many experiments and therefore we decided to test it at a higher level. We performed a series of *in vitro* aggregation assays to reveal the aggregation properties of fucosylated compounds towards *P. asymbiotica* subsp. *australis*. Prior to each assay, we confirmed the absence of aggregates in the negative control – bacterial cells in 50% DMSO (Figure 8A). We studied mono-, di-, tri- and tetravalent fucoclusters as ligands (Table 5, Figure 8). The monovalent compound **5** did not create any aggregates, as expected. With all multivalent compounds, we observed bacterial aggregates of spherical shape and variable size that confirmed that all multivalent compounds are capable of interacting with a cell surface's receptors. The concentration of the first appearance of aggregates varied according to the nature of the ligand used (Figure 8C). The highest efficiency (0.63 mM) was observed for the trifucosylated compound **16**. Against our expectations, it was higher than for tetrameric fucoclusters (compounds **18** and **20**) that aggregated cells at a concentration of 5 mM. A similar result was obtained for the other trivalent compound **19**. This could be caused by the structure of compound **16**, its longer linker arms allow a higher flexibility of the compound and easier reach on different cells.

Table 5. The determination of the minimal concentration of multivalent fucoclusters able to aggregate *P. asymbiotica* cells.

Ligand	The lowest concentration able to aggregate <i>P. asymbiotica</i> cells
Compound 5	No visible aggregation in used concentration
Compound 24	5 mM
Compound 19	2.5 mM
Compound 20	2.5 mM
Compound 18	2.5 mM
Compound 16	0.63 mM

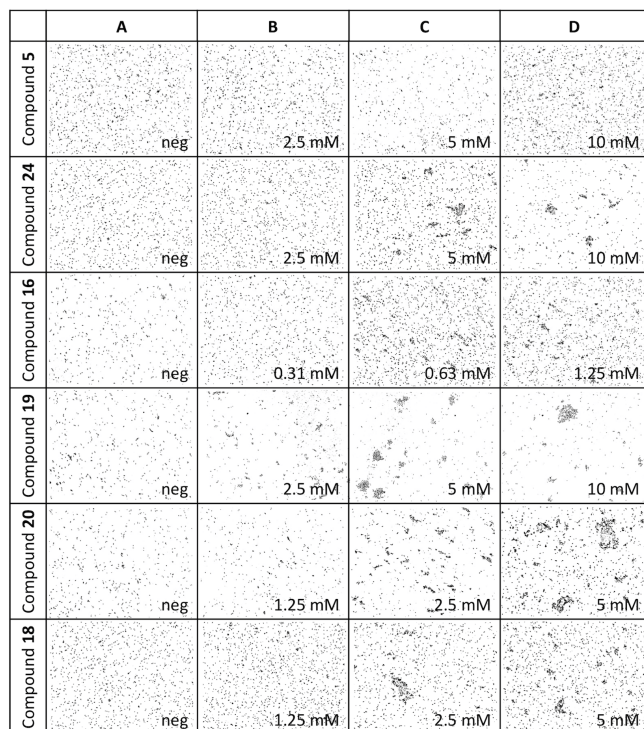


Figure 8. Representative images of optical microscopy observation (200x) of bacterial cell aggregation for *Photobacterium asymbiotica* subsp. *australis* with different fucosylated clusters. Mixture with 50% DMSO was used as negative control (A). Concentrations of the first appearance of aggregates are presented (C) as well as one dilution step lower (B) and higher (D). No aggregates were observed for a monovalent fucocluster (compound 5). Background of all pictures was subtracted in GIMP software.

Conclusions

P. asymbiotica has proved to be not only an entomopathogenic bacteria, but also a dangerous human pathogen that causes a difficult-to-treat disease. Suitable inhibitors preventing the host-pathogen interaction should be helpful in the early steps of *P. asymbiotica* infection. For this purpose, monovalent fucosides and di-, tri-, and tetravalent glycoclusters functionalized with α -L-fucosides were designed and prepared using click chemistry. Their binding properties toward the PHL lectin from *P. asymbiotica* have been evaluated by hemagglutination, ITC, SPR, NMR, X-ray crystallography, and cell cross-linking.

We have demonstrated that all of the compounds were able to inhibit the PHL binding activity and the affinity for multivalent ligands reached nanomolar values, and there is an obvious relation between the increasing number of fucoses per cluster and increasing affinity. The potency of ligands depended on the valency, architecture and flexibility of the fucocluster, but all ligands proved to be up to several orders of magnitude better ligands than L-fucose. Moreover, only multivalent ligands were able to cross-link PHL, resulting in the formation of visible precipitation. We used this property and investigated the agglutination of *P. asymbiotica* bacteria via the surface lectins that are likely present, as was proved for other cells (e.g. *P.*

aeruginosa, *E. coli*, T cell leukemia line).^[18–20] We observed nice cell clumps at different concentrations of multivalent compounds, showing the specificity of the interaction and proving the presence of lectins on the bacterial surface. In conclusion, we provide complete assays of the action of mono- and multivalent fucoclusters on the *P. asymbiotica* lectin PHL and useful information for their possible employment in medical treatments.

Experimental Section

Synthesis - General methods

Optical rotations were measured at room temperature with a Perkin-Elmer 241 automatic polarimeter. TLC analysis was performed on Kieselgel 60 F₂₅₄ (Merck, Germany) silica gel plates with visualization by immersing in a sulfuric-acid solution (5% in EtOH) followed by heating. Column chromatography was performed on silica gel 60 (0.063–0.200 mm, Merck, Germany), flash column chromatography was performed on silica gel 60 (Merck 0.040–0.063 mm). Gel filtration was performed on Sephadex G-25 (Sigma-Aldrich, USA), using methanol as the eluent. Organic solutions were dried over MgSO₄ and concentrated under vacuum. The ¹H (400 MHz) and ¹³C NMR (100.28 MHz) spectra were recorded with Bruker Avance II 400 spectrometer (Bruker, Germany). Chemical shifts are referenced to Me₄Si or DSS (0.00 ppm for ¹H) and to solvent signals (CDCl₃: 77.00 ppm, CD₃OD: 49.15 ppm, DMSO-d₆: 39.51 ppm for ¹³C). MS (MALDI-TOF) analysis was carried out in positive reflection mode with a BIFLEX III mass spectrometer (Bruker, Germany) with delayed-ion extraction. The matrix solution was a saturated solution of 2,5-dihydroxy-benzoic acid (DHB) in DMF. Elemental analysis was performed on an Elementar Vario MicroCube instrument (Elementar UK Ltd., UK).

General method A for azide-alkyne click reaction. Et₃N (1 equiv./alkyne) and copper(I)-iodide (0.1 equiv./alkyne) were added to a stirred solution of alkyne (0.2 mmol) and azide (1.3 equiv./alkyne) in CH₃CN (3 mL) under an argon atmosphere and stirred overnight at room temperature. The reaction mixture was evaporated, and the crude product was purified by flash column chromatography to give the desired compound.

General method B for nucleophilic substitution of tosylates to azide. NaN₃ (2 equiv.) was added to a stirred solution of tosylate (1 mmol) in DMF (5 mL) under an argon atmosphere and stirred overnight at room temperature. The reaction mixture was diluted with water dropwise, stirred for further 5 minutes and evaporated. The residue was dissolved in CH₂Cl₂ (200 mL) and extracted with water (2 x 50 mL) and brine (50 mL), dried over MgSO₄, filtered and evaporated. The crude product was purified by flash column chromatography to give the desired compound.

General method C for Zemplén-deacetylation. The catalytic amount of NaOMe (pH ~ 9) was added to a stirred solution of ester (0.2 mmol) in dry MeOH (5 mL) and stirred overnight at room temperature. The reaction mixture was neutralized with Amberlite IR-120 H⁺ ion-exchange resin, filtered and evaporated, and then the crude product was purified by flash column chromatography and gel filtration to give the desired compound.

Compound 8. Azide compound 3 (637 mg, 1.71 mmol) and alkyne 1 (131 mg, 0.44 mmol) were reacted in CH₃CN according to general method A. The crude product was purified by flash column chromatography (CH₂Cl₂/MeOH 98:2) to give compound 7 (540 mg, 87%) as a colourless syrup. *R*_f = 0.50 (CH₂Cl₂/MeOH 97:3). The product

7 (540 mg, 0.38 mmol) was converted into azide according to general method **B**. The crude product was purified by flash column chromatography (CH₂Cl₂/MeOH 95:5) to give compound **8** (254 mg, 65%) as a colourless syrup. *R*_f = 0.39 (CH₂Cl₂/MeOH 95:5); ¹H NMR (400 MHz, CDCl₃): δ = 7.96, 7.89 (2 x s, 3H, 3 x CH triazole), 7.44 (s, 2H, arom), 5.24 (d, *J* = 1.8 Hz, 6H, 3 x CH₂ propargyl), 4.58 (t, *J* = 5.1 Hz, 4H, 2 x NCH₂ TEG), 4.51 (t, *J* = 5.3 Hz, 2H, NCH₂ TEG), 3.92-3.85 (m, 10H, 5 x OCH₂ TEG), 3.65-3.58 (m, 29H, 13 x OCH₂ TEG, COOCH₃), 3.37-3.35 (m, 6H, 3 x CH₂ TEG) ppm; ¹³C NMR (100 MHz, CDCl₃): δ = 166.3 (1C, COOCH₃), 152.0 (2C, C_q arom.), 144.0, 143.1 (3C, 3 x C_q triazole), 141.6 (1C, C_q arom.), 125.5 (1C, C_q arom.), 124.8, 124.4 (3C, 3 x CH triazole), 109.1 (2C, arom.), 70.6, 70.5, 69.9, 69.3, 69.2 (18C, 18 x CH₂ TEG), 66.4, 63.1 (3C, 3 x CH₂ propargyl), 52.3 (1C, COOCH₃), 50.6, 50.2, 50.0 (6C, 6 x NCH₂ TEG) ppm. MS (MALDI-TOF): *m/z* calcd for C₄₁H₆₂N₁₈NaO₁₄: 1054.05 [M+Na]⁺; found: 1053.79; elemental analysis calcd (%) for C₄₁H₆₂N₁₈O₁₄: C 47.76, H 6.06; found: C 47.81, H 6.12.

Compound 10. Azide compound **4** (626 mg, 2.59 mmol) and alkyne **1** (199 mg, 0.67 mmol) were reacted in CH₃CN according to general method **A**. The crude product was purified by flash column chromatography (CH₂Cl₂/MeOH 97:3) to give compound **9** (700 mg, 88%) as a colourless syrup. *R*_f = 0.18 (CH₂Cl₂/MeOH 97:3). Compound **9** (474 mg, 0.5 mmol) was converted into azide according to general method **B**. The crude product was purified by flash column chromatography (CH₂Cl₂/MeOH 97:3) to give compound **10** (175 mg, 58%) as a colourless syrup. [α]_D²⁴ +1.3 (*c* = 0.15, CHCl₃); *R*_f = 0.48 (CH₂Cl₂/MeOH 95:5); ¹H NMR (400 MHz, CDCl₃): δ = 7.97 (s, 3H, 3 x CH triazole), 7.41 (s, 2H, arom.), 5.31 (d, *J* = 1.3 Hz, 2H, CH₂ propargyl), 5.25 (s, 4H, 2 x CH₂ propargyl), 4.55-4.51 (m, 6H, 3 x NCH₂ ethylene glycol), 3.88-3.80 (m, 9H, 3 x CH₂ ethylene glycol, COOCH₃) ppm; ¹³C NMR (100 MHz, CDCl₃): δ = 166.0 (1C, COOCH₃), 151.6 (1C, C_q arom.), 144.2, 143.4 (3C, 3 x C_q triazole), 141.1 (1C, C_q arom.), 125.5 (1C, C_q arom.), 124.6, 124.1 (3C, 3 x CH triazole), 108.8 (2C, arom.), 66.0, 62.7 (3C, 3 x CH₂ propargyl), 52.1 (1C, COOCH₃), 50.3, 49.2, 49.0 (6C, 6 x NCH₂ ethylene glycol) ppm. MS (MALDI-TOF): *m/z* calcd for C₂₃H₂₆N₁₈NaO₅: 657.22 [M+Na]⁺; found: 657.14; elemental analysis calcd (%) for C₂₃H₂₆N₁₈O₅: C 43.53, H 4.13; found: C 43.59, H 4.21.

Compound 12. Azide compound **3** (850 mg, 2.27 mmol) and alkyne **2** (126mg, 0.44 mmol) were reacted in CH₃CN according to general method **A**. The crude product was purified by flash column chromatography (CH₂Cl₂/MeOH 97:3) to give compound **11** (474 mg, 61%) as a colourless syrup. *R*_f = 0.29 (CH₂Cl₂/MeOH 97:3). Compound **11** (474 mg, 0.27 mmol) was converted into azide according to general method **B**. The crude product was purified by flash column chromatography (CH₂Cl₂/MeOH 95:5) to give compound **12** (337 mg, 51%) as a colourless syrup. *R*_f = 0.12 (CH₂Cl₂/MeOH 95:5); ¹H NMR (400 MHz, CDCl₃): δ = 7.73 (s, 4H, 4 x CH triazole), 4.55-4.53 (m, 16H, 4 x CH₂ propargyl, 4 x NCH₂ TEG), 3.89 (t, *J* = 5.2 Hz, 8H, 4 x OCH₂ TEG), 3.68-3.62 (m, 40H, 20 x OCH₂ TEG), 3.48 (s, 8H, 4 x CH₂ pentaerythrit), 3.39-3.37 (m, 8H, 4 x CH₂ TEG) ppm; ¹³C NMR (100 MHz, CDCl₃): δ = 145.1 (4C, 4 x C_q triazole), 123.7 (4C, 4 x CH triazole), 70.7, 70.6, 70.5, 70.0, 69.5 (24C, 24 x OCH₂ TEG), 69.2 (4C, 4 x CH₂ pentaerythrit), 64.9 (4C, 4 x CH₂ propargyl), 50.6, 50.1 (8C, 8 x NCH₂ TEG), 45.3 (1C, C_q pentaerythrit) ppm. MS (MALDI-TOF): *m/z* calcd for C₄₉H₈₄N₂₄NaO₁₆: 1287.64 [M+Na]⁺; found: 1287.91; elemental analysis calcd (%) for C₄₉H₈₄N₂₄O₁₆: C 46.51, H 6.69; found: C 46.56, H 6.75.

Compound 14. Azide compound **4** (834 mg, 3.46 mmol) and alkyne **2** (192 mg, 0.67 mmol) were reacted in CH₃CN according to general method **A**. The crude product was purified by flash column chromatography (CH₂Cl₂/MeOH 95:5) to give compound **13** (430 mg, 42%) as a colourless syrup. *R*_f = 0.22 (CH₂Cl₂/MeOH 95:5). Compound **13** (420 mg, 0.34 mmol) was converted into azide according to general

method **B**. The crude product was purified by flash column chromatography (CH₂Cl₂/MeOH 95:5) to give compound **14** (238 mg, 94%) as a colourless syrup. [α]_D²⁴ +16.1 (*c* = 0.18, CHCl₃); *R*_f = 0.24 (CH₂Cl₂/MeOH 95:5); ¹H NMR (400 MHz, CDCl₃): δ = 7.77 (s, 4H, 4 x CH triazole), 4.59 (s, 8H, 4 x CH₂ propargyl), 4.56-4.53 (m, 8H, 4 x NCH₂ TEG), 3.84-3.81 (m, 8H, 4 x CH₂ TEG), 3.48 (s, 8H, 4 x CH₂ pentaerythrit) ppm; ¹³C NMR (100 MHz, CDCl₃): δ = 145.4 (4C, 4 x C_q triazole), 123.4 (4C, 4 x CH triazole), 69.0 (4C, 4 x CH₂ pentaerythrit), 64.7 (4C, 4 x CH₂ propargyl), 50.5, 49.2 (8C, 8 x NCH₂ TEG), 45.1 (1C, C_q pentaerythrit) ppm. MS (MALDI-TOF): *m/z* calcd for C₂₅H₃₆N₂₄NaO₄: 759.32 [M+Na]⁺; found: 759.53; elemental analysis calcd (%) for C₂₅H₃₆N₂₄O₄: C 40.76, H 4.93; found: C 40.82, H 5.03.

Compound 15. Azide compound **8** (100 mg, 0.10 mmol) and alkyne **6** (143 mg, 0.44 mmol) were reacted in CH₃CN according to general method **A**. The crude product was purified by flash column chromatography (CH₂Cl₂/MeOH 95:5) to give compound **15** (96 mg, 49%) as a colourless syrup. [α]_D²⁴ -77.9 (*c* = 0.05, CHCl₃); *R*_f = 0.28 (CH₂Cl₂/MeOH 95:5); ¹H NMR (400 MHz, CDCl₃): δ = 7.95, 7.72, 7.71 (3 x s, 6H, 6 x CH triazole), 7.44 (s, 2H, arom.), 5.36-5.26 (m, 12H, 3 x CH₂ propargyl, 3 x H-3, 3 x H-4), 5.18 (d, *J* = 3.6 Hz, 3H, 3 x H-1), 5.12 (dd, *J* = 10.8 Hz, *J* = 3.7 Hz, 3H, 3 x H-2), 4.82 (d, *J* = 12.4 Hz, 3H, 3 x CH_{2a} propargyl), 4.66 (d, *J* = 12.4 Hz, 3H, 3 x CH_{2b} propargyl), 4.53-4.51 (m, 12H, 6 x NCH₂ TEG), 4.21 (q, *J* = 6.4 Hz, 3H, 3 x H-5), 3.90-3.84 (m, 15H, 6 x OCH₂ TEG, COOCH₃), 3.61-3.56 (m, 24H, 12 x OCH₂ TEG), 2.16, 2.02, 1.96 (3 x s, 27H, 9 x CH₃ Ac), 1.13 (d, *J* = 6.5 Hz, 9H, 3 x CH₃) ppm; ¹³C NMR (100 MHz, CDCl₃): δ = 170.6, 170.4, 170.0 (9C, 9 x CO Ac), 166.3 (1C, COOCH₃), 152.0 (2C, 2 x C_q arom.), 143.8, 142.9 (6C, 6 x C_q triazole), 141.6 (1C, C_q arom.), 125.7 (1C, C_q arom.), 124.6, 124.0 (6C, 6 x CH triazole), 109.2 (2C, arom.), 95.7 (3C, 3 x C-1), 71.2, 68.0, 67.9, 64.7 (12C, skeleton carbons), 70.5, 70.4, 69.4, 69.3 (18C, 18 x OCH₂ TEG), 66.3, 62.8, 61.3 (6C, 6 x CH₂ propargyl), 52.4 (1C, COOCH₃), 50.4, 50.3 (6C, 6 x NCH₂ TEG), 20.8, 20.7, 20.6 (9C, 9 x CH₃ Ac), 15.9 (3C, 3 x CH₃); ppm. MS (MALDI-TOF) *m/z* calcd for C₈₆H₁₂₂N₁₈NaO₃₈: 2037.81 [M+Na]⁺ found: 2037.80; elemental analysis calcd (%) for C₈₆H₁₂₂N₁₈O₃₈: C 51.24, H 6.10; found: C 51.31, H 6.19.

Compound 16. Method I: Azide compound **8** (57 mg, 0.06 mmol) and alkyne **5** (50 mg, 0.25 mmol) were reacted in CH₃CN according to general method **A**. The crude product was purified by flash column chromatography (CH₃CN/H₂O 7:3) to give compound **16** (54 mg, 60%) as a colourless syrup. **Method II:** Compound **15** (74 mg, 0.04 mmol) was deacetylated according to general method **C**. The crude product was purified by flash column chromatography (CH₂Cl₂/MeOH 7:3) to give compound **16** (47 mg, 78%) as a colourless syrup. [α]_D²⁴ +173.0 (*c* = 0.10, MeOH); *R*_f = 0.42 (CH₂Cl₂/MeOH 7:3); ¹H NMR (400 MHz, D₂O): δ = 8.06, 7.94, 7.80 (3 x s, 6H, 6 x CH triazole), 7.38 (s, 2H, arom.), 5.14, 5.08 (2 x s, 6H, 3 x CH₂ propargyl), 4.89 (d, *J* = 2.9 Hz, 3H, 3 x H-1), 4.61 (dd, *J* = 22.7 Hz, *J* = 13.3 Hz, 6H, 3 x CH₂ propargyl), 4.57-4.44 (m, 12H, 6 x NCH₂ TEG), 3.85-3.75 (m, 18H, 3 x H-5, 6 x OCH₂ TEG, COOCH₃), 3.71-3.70 (m, 6H, 3 x H-2, 3 x H-3), 3.66 (s, 3H, 3 x H-4), 3.46-3.42 (m, 12H, 6 x OCH₂ TEG), 3.41-3.39 (m, 12H, 6 x OCH₂ TEG), 1.02 (d, *J* = 6.5 Hz, 9H, 3 x CH₃); ¹³C NMR (100 MHz, D₂O): δ = 168.7 (1C, COOCH₃), 152.5 (2C, 2 x C_q arom.), 145.0, 143.8 (6C, 6 x C_q triazole), 141.3 (1C, C_q arom.), 126.7 (1C, C_q arom.), 126.6, 126.1 (6C, 6 x CH triazole), 110.2 (2C, arom.), 99.5 (3C, 3 x C-1), 72.8 (3C, 3 x C-4), 70.6 (3C, 3 x C-2), 70.7, 70.5, 69.7, 69.6 (18C, 18 x OCH₂ TEG), 69.0 (3C, 3 x C-3), 67.7 (3C, 3 x C-5), 66.0, 62.9, 61.5 (6C, 6 x CH₂ propargyl), 53.8 (1C, COOCH₃), 51.1, 51.0, 50.9 (6C, 6 x NCH₂ TEG), 16.2 (3C, 3 x CH₃). MS (MALDI-TOF): *m/z* calcd for C₆₈H₁₀₄N₁₈NaO₂₉: 1659.71 [M+Na]⁺; found: 1659.80; elemental analysis calcd (%) for C₆₈H₁₀₄N₁₈O₂₉: C 49.87, H 6.40; found: C 49.92, H 6.50.

Compound 17. Azide compound **12** (85 mg, 0.05 mmol) and alkyne **6** (94 mg, 0.28 mmol) were reacted in CH₃CN according to general method **A**. The crude product was purified by flash column chromatography (CH₂Cl₂/MeOH 95:5) to give compound **17** (80 mg, 54%) as a colourless syrup. [α]_D²⁴ -70.0 (*c* = 0.31, CHCl₃); *R*_f = 0.22 (CH₂Cl₂/MeOH 95:5); ¹H NMR (400 MHz, CDCl₃): δ = 7.74, 7.73 (2 x s, 8H, 8 x CH triazole), 5.34 (dd, *J* = 10.8 Hz, *J* = 3.3 Hz, 4H, 4 x H-3), 5.28 (d, *J* = 2.7 Hz, 4H, 4 x H-4), 5.18 (d, *J* = 3.7 Hz, 4H, 4 x H-1), 5.12 (dd, *J* = 10.8 Hz, *J* = 3.7 Hz, 4H, 4 x H-2), 4.82 (d, *J* = 12.4 Hz, 4H, 4 x CH_{2a} propargyl), 4.66 (d, *J* = 12.4 Hz, 4H, 4 x CH_{2b} propargyl), 4.55-4.52 (m, 24H, 8 x NCH₂ TEG, 4 x CH₂ propargyl), 4.22 (q, *J* = 6.4 Hz, 4H, 4 x H-5), 3.88 (t, *J* = 5.1 Hz, 16H, 8 x OCH₂ TEG), 3.61-3.57 (m, 32H, 16 x OCH₂TEG), 3.48 (s, 8H, 4 x CH₂ pentaerythrit), 2.16, 2.03, 2.01, 1.97 (4 x s, 36H, 12 x CH₃ Ac), 1.13 (d, *J* = 6.5 Hz, 12H, 4 x CH₃); ¹³C NMR (100 MHz, CDCl₃): δ = 170.4, 170.2, 169.8 (9C, 9 x CO Ac), 144.8, 143.6 (8C, 8 x C_q triazole), 123.8 (8C, 8 x CH triazole), 95.5 (4C, 4 x C-1), 71.0, 67.8, 67.7, 64.5 (16C, 4 x skeleton carbons), 70.3, 69.2, (24C, 24 x OCH₂ TEG), 69.0 (4C, 4 x CH₂ pentaerythrit), 64.6 (4C, 4 x CH₂ propargyl), 61.1 (4C, 4 x CH₂ propargyl), 50.1, 50.0 (8C, 8 x NCH₂ TEG), 45.3 (1C, C_q pentaerythrit), 20.6, 20.5 (12C, 12 x CH₃ Ac), 15.7 (4C, 4 x CH₃). MS (MALDI-TOF): *m/z* calcd for C₁₀₉H₁₆₄N₂₄NaO₄₈: 2600.10 [*M*+Na]⁺; found: 2600.13; elemental analysis calcd (%) for C₁₀₉H₁₆₄N₂₄O₄₈: C 50.77, H 6.41; found: C 50.83, H 6.49.

Compound 18. Method I: Azide compound **12** (85 mg, 0.07 mmol) and alkyne **5** (82 mg, 0.40 mmol) were reacted in CH₃CN according to general method **A**. The crude product was purified by flash column chromatography (CH₃CN/H₂O 7:3) to give compound **18** (91 mg, 65%) as a colourless syrup. **Method II:** Compound **17** (82 mg, 0.03 mmol) was deacetylated according to general method **C**. The crude product was purified by flash column chromatography (CH₃CN/H₂O 7:3) to give compound **18** (37 mg, 60%) as a colourless syrup. [α]_D²⁴ -91.1 (*c* = 0.09, MeOH); *R*_f = 0.18 (CH₃CN/H₂O 7:3); ¹H NMR (400 MHz, D₂O): δ = 7.98, 7.90 (2 x s, 8H, 8 x CH triazole), 4.91 (d, *J* = 3.4 Hz, 4H, 4 x H-1), 4.65 (q, *J* = 12.8 Hz, 8H, 4 x CH₂ propargyl), 4.54-4.49 (m, 16H, 8 x NCH₂ TEG), 4.41 (s, 8H, 4 x CH₂ propargyl), 3.87-3.83 (m, 20H, 4 x H-5, 8 x OCH₂ TEG), 3.72 (dd, *J* = 7.4 Hz, *J* = 3.3 Hz, 8H, 4 x H-2, 4 x H-3), 3.69-3.68 (m, 4H, 4 x H-4), 3.51-3.49 (m, 16H, 8 x OCH₂ TEG), 3.44-3.43 (m, 16H, 8 x OCH₂ TEG), 3.30 (s, 8H, 4 x CH₂ pentaerythrit), 1.03 (d, *J* = 6.6 Hz, 12H, 4 x CH₃); ¹³C NMR (100 MHz, D₂O): δ = 145.1, 145.0 (8C, 8 x C_q triazole), 126.2, 126.1 (8C, 8 x CH triazole), 99.5 (4C, 4 x C-1), 72.7 (4C, 4 x C-4), 70.5 (4C, 4 x C-2), 70.6, 70.5, 70.4, 69.7 (24C, 24 x OCH₂ TEG), 69.2 (4C, 4 x CH₂ pentaerythrit), 68.9 (4C, 4 x C-3), 67.7 (4C, 4 x C-5), 64.5 (4C, 4 x CH₂ propargyl), 61.6 (4C, 4 x CH₂ propargyl), 51.0 (8C, 8 x NCH₂ TEG), 45.6 (1C, C_q pentaerythrit), 16.2 (4C, 4 x CH₃). MS (MALDI-TOF): *m/z* calcd for C₈₅H₁₄₀N₂₄NaO₃₆: 2097.15 [*M*+Na]⁺; found: 2097.24; elemental analysis calcd (%) for C₈₅H₁₄₀N₂₄O₃₆: C 49.22, H 6.80; found: C 49.31, H 6.94.

Compound 19. Azide compound **10** (50 mg, 0.08 mmol) and alkyne **5** (72 mg, 0.36 mmol) were reacted in CH₃CN according to general method **A**. The crude product was purified by flash column chromatography (CH₃CN/H₂O 7:3) to give compound **19** (70 mg, 71%) as a colourless syrup. [α]_D²⁴ -67.5 (*c* = 0.16, H₂O); *R*_f = 0.54 (CH₃CN/H₂O 7:3); ¹H NMR (400 MHz, D₂O): δ = 7.87, 7.75, 7.69 (3 x s, 6H, 6 x CH triazole), 7.16 (s, 2H, arom.), 4.99, 4.93 (2 x s, 6H, 3 x CH₂ propargyl), 4.88 (s, 8H, 4 x NCH₂ ethylene glycol), 4.80 (s, 7H, 2 x NCH₂ ethylene glycol, 3 x H-1), 4.47 (dd, *J* = 27.0 Hz, *J* = 12.1 Hz, 6H, 3 x CH₂ propargyl), 3.77 (s, 3H, COOCH₃), 3.76-3.61 (m, 12H, 3 x H-5, 3 x H-2, 3 x H-3, 3 x H-4), 0.95 (d, *J* = 6.4 Hz, 9H, 3 x CH₃) ppm; ¹³C NMR (100 MHz, D₂O): δ = 166.6 (1C, COOCH₃), 150.3 (2C, 2 x C_q arom.), 143.4 (6C, 6 x C_q triazole), 139.2 (1C, C_q arom.), 124.6 (1C, C_q arom.), 124.0 (6C, 6 x CH triazole), 108.1 (2C, arom.), 97.5 (3C, 3 x C-1), 70.9 (3C, 3 x C-4), 67.1 (3C, 3 x C-2), 65.9 (3C, 3 x C-3), 64.1 (3C, 3 x C-5), 63.8, 60.9, 59.4 (6C, 6 x CH₂ propargyl), 52.1 (1C, COOCH₃), 49.0 (6C, 6 x NCH₂ ethylene glycol),

14.4 (3C, 3 x CH₃) ppm. MS (MALDI-TOF): *m/z* calcd for C₅₀H₆₈N₁₈NaO₂₀: 1263.48 [*M*+Na]⁺; found: 1263.50; elemental analysis calcd (%) for C₅₀H₆₈N₁₈O₂₀: C 48.38, H 5.52; found: C 48.44, H 5.61.

Compound 20. Azide compound **14** (105 mg, 0.14 mmol) and alkyne **5** (170 mg, 0.84 mmol) were reacted in CH₃CN according to general method **A**. The crude product was purified by flash column chromatography (CH₃CN/H₂O 7:3) to give compound **20** (102 mg, 46%) as a colourless syrup. [α]_D²⁴ -64.6 (*c* = 0.11, H₂O); *R*_f = 0.29 (CH₃CN/H₂O 7:3); ¹H NMR (400 MHz, D₂O): δ = 7.81, 7.75 (2 x s, 8H, 8 x CH triazole), 4.84 (s, 16H, 8 x NCH₂ ethylene glycol), 4.78 (s, 4H, 4 x H-1), 4.52 (dd, *J* = 28.9 Hz, *J* = 12.6 Hz, 8H, 4 x CH₂ propargyl), 4.33 (s, 8H, 4 x CH₂ propargyl), 3.76 (d, *J* = 6.4 Hz, 4H, 4 x H-5), 3.64 (s, 8H, 4 x H-2, 4 x H-3), 3.60 (s, 4H, 4 x H-4), 3.19 (s, 8H, 4 x CH₂ pentaerythrit), 0.95 (d, *J* = 6.4 Hz, 12H, 4 x CH₃) ppm; ¹³C NMR (100 MHz, D₂O): δ = 145.4, 145.2 (8C, 8 x C_q triazole), 126.1, 126.0 (8C, 8 x CH triazole), 99.4 (4C, 4 x C-1), 72.8 (4C, 4 x C-4), 70.6 (4C, 4 x C-2), 69.4 (4C, 4 x CH₂ pentaerythrit), 69.0 (4C, 4 x C-3), 67.7 (4C, 4 x C-5), 64.4 (4C, 4 x CH₂ propargyl), 61.2 (4C, 4 x CH₂ propargyl), 50.8 (8C, 8 x NCH₂ ethylene glycol), 45.6 (1C, C_q pentaerythrit), 16.3 (4C, 4 x CH₃) ppm. MS (MALDI-TOF): *m/z* calcd for C₆₁H₉₂N₂₄NaO₂₄: 1567.66 [*M*+Na]⁺; found: 1567.65; elemental analysis calcd (%) for C₆₁H₉₂N₂₄O₂₄: C 47.41, H 6.00; found: C 47.49, H 6.08.

Compound 22. Azide compound **4** (180 mg, 0.75 mmol) and alkyne **5** (101 mg, 0.50 mmol) were reacted in CH₃CN according to general method **A**. The crude product was purified by flash column chromatography (CH₂Cl₂/MeOH 9:1) and the product was converted into azide according to general method **B**. The crude product was purified by flash column chromatography (CH₂Cl₂/MeOH 9:1) to give compound **22** (77 mg, 49%) as a colourless syrup. [α]_D²⁴ -132.6 (*c* = 0.12, H₂O); *R*_f = 0.38 (CH₂Cl₂/MeOH 85:15); ¹H NMR (400 MHz, CDCl₃+CD₃OD): δ = 7.91 (s, 1H, CH triazole), 4.94 (s, 1H, H-1), 4.83 (d, *J* = 12.6 Hz, 1H, CH_{2a} propargyl), 4.67 (d, *J* = 12.5 Hz, 1H, CH_{2b} propargyl), 4.57-4.54 (m, 2H, NCH₂ ethylene glycol), 3.98 (q, *J* = 6.5 Hz, 1H, H-5), 3.86-3.83 (m, 2H, N₃CH₂ ethylene glycol), 3.78 (s, 2H, H-2, H-3), 3.71 (s, 1H, H-4), 1.26 (d, *J* = 6.6 Hz, 3H, CH₃) ppm; ¹³C NMR (100 MHz, CDCl₃+CD₃OD): δ = 144.2 (1C, C_q triazole), 123.7 (1C, CH triazole), 98.2 (1C, C-1), 71.6, 70.0, 68.4, 66.1 (4C, C-2, C-3, C-4, C-5), 60.2 (1C, CH₂ propargyl), 50.1, 49.1 (2C, 2 x NCH₂ ethylene glycol), 15.4 (1C, CH₃) ppm. MS (MALDI-TOF): *m/z* calcd for C₁₁H₁₈N₆NaO₅: 337.12 [*M*+Na]⁺; found: 337.26; elemental analysis calcd (%) for C₁₁H₁₈N₆O₅: C 42.04, H 5.77; found: C 42.11, H 5.83.

Compound 23. Diazide compound **21** (312 mg, 1.28 mmol) and alkyne **5** (72 mg, 0.36 mmol) were reacted in CH₃CN according to general method **A**. The crude product was purified by flash column chromatography (CH₂Cl₂/MeOH 9:1→7:3) to give compound **23** (56 mg, 35%) as a colourless syrup. (The dimer compound **24** was also observed). [α]_D²⁴ -87.1 (*c* = 0.16, H₂O); *R*_f = 0.42 (CH₂Cl₂/MeOH 7:3); ¹H NMR (400 MHz, CDCl₃): δ = 7.83 (s, 1H, CH triazole), 4.94 (s, 1H, H-1), 4.79 (d, *J* = 12.3 Hz, 1H, CH_{2a} propargyl), 4.64 (d, *J* = 12.5 Hz, 1H, CH_{2b} propargyl), 4.54 (s, 2H, NCH₂ TEG), 3.96-3.94 (m, 1H, H-5), 3.88-3.84 (m, 4H, OCH₂ TEG, H-2, H-3), 3.75 (s, 1H, H-4), 3.68-3.62 (m, 10H, 5 x OCH₂ TEG), 3.40-3.37 (m, 2H, N₃CH₂ TEG), 1.23 (d *J* = 6.2 Hz, 3H, CH₃) ppm; ¹³C NMR (100 MHz, CDCl₃): δ = 144.1 (1C, C_q triazole), 124.2 (1C, CH triazole), 98.5 (1C, C-1), 72.1, 70.7, 68.9, 66.5 (4C, C-2, C-3, C-4, C-5), 70.6, 70.5, 70.1, 69.4 (6C, 6 x OCH₂ TEG), 60.8 (1C, CH₂ propargyl), 50.7, 50.3 (2C, 2 x NCH₂ TEG), 16.3 (1C, CH₃) ppm. MS (MALDI-TOF): *m/z* calcd for C₁₇H₃₀N₆NaO₈: 469.20 [*M*+Na]⁺; found: 469.24; elemental analysis calcd (%) for C₁₇H₃₀N₆O₈: C 45.73, H 6.77; found: C 45.81, H 6.88.

Ligand preparation

All lyophilized ligands were dissolved in DMSO to final concentration 50 mM and used in selected assays.

Protein production and purification

Protein was produced in *Escherichia coli* Tuner(DE3)/pET25b_phl cells as previously described.^[5] The cells were grown in LB broth medium containing 100 μ M ampicillin at 37 °C. When the culture reached an OD₆₀₀ of 0.5, protein production was induced with 0.2 mM isopropyl β -D-1-thiogalactopyranoside (IPTG, ForMedium, UK). Cells were incubated for an additional 20 hours at 18 °C, harvested by centrifugation at 12,000 g for 10 min and resuspended in buffer A (20 mM Tris/HCl, 300 mM NaCl, pH 7.5). Harvested cells were stored at -20 °C prior to protein purification.

Cells were then disintegrated by sonication (VCX 500, Sonics & Materials, Inc., USA) and the cytosolic fraction containing soluble PHL was collected by centrifugation at 21,000 g at 4 °C for 1 hour and filtrated through a 0.45 μ m pore size filter (Carl Roth, Germany). Recombinant protein PHL was purified with isocratic elution on a d-mannose-agarose (Sigma-Aldrich, USA) resin equilibrated with buffer A by affinity chromatography using an ÄKTA FPLC system (GE Healthcare, UK). Purified PHL was dialyzed against appropriate buffer and used for further studies.

Hemagglutination inhibition assay

Human red blood cells (RBCs) O were processed according to previously published work.^[5] In brief, RBCs O treated with natrium citrate were washed four times by PBS buffer (137 mM NaCl, 2.7 mM KCl, 8 mM Na₂HPO₄, 1.47 mM KH₂PO₄, pH 7.4), diluted to 50% by PBS with 0.005% (w/w) natrium azide and treated by 0.1% papain for the duration of 30 minutes. IRB approval for use of these samples is not requested.

Hemagglutination inhibition assay was performed for specificity and semi-quantitative affinity of the PHL interaction with the compounds. Chosen carbohydrate inhibitors in starting concentration from 12.5 mM to 0.1 mM were used for determination of the lowest inhibiting concentration. The lectin in concentration 2 mg mL⁻¹ was mixed with serially diluted carbohydrate inhibitors in a 5 μ l:5 μ l ratio. Subsequently, 10 μ l of 10% RBCs O was added. The mixture was thoroughly mixed and incubated for 10 minutes at room temperature.^[21] After incubation, mixture was again mixed and reaction was observed on microscope slides using Levenhuk 2L NG microscope with Levenhuk D2L digital camera (Levenhuk, USA). For obtaining images, the software ToupView for Windows (Levenhuk, USA) was used. The positive (PHL without inhibitor) and negative control (reaction without PHL) were prepared and processed in the same way using the appropriate volume of PBS buffer instead of the not included components. The lowest concentration of inhibitor able to inhibit agglutination was determined and compared with the standard (L-fucose).

Surface plasmon resonance

Surface plasmon resonance (SPR) experiments were performed on a BIAcore T200 instrument (GE Healthcare, UK) at 25 °C, using buffer A supplemented with 0.05 % Tween 20 as a running buffer. α -L-fucoside was immobilized onto CM5 sensor chip (GE Healthcare, UK) covered with a carboxymethylated dextran matrix. The sensor chip surface was activated with *N*-ethyl-*N*-(3-dimethylaminopropyl)carbodiimide/*N*-hydroxysuccinimide solution and then coated with streptavidin using the manufacturer's standard protocol using HBS buffer (10 mM HEPES, 150 mM NaCl, 0.05% Tween 20, pH 7.5). Unreacted groups were blocked with 1 M ethanolamine-HCl, pH 8.5. Biotinylated carbohydrate (biotin-

PAA-monosaccharides, Lectinity, Russia) was injected onto particular measuring channel and pure biotin on blank channel at a flow rate of 5 μ l min⁻¹.

In the experimental setup, SPR inhibition measurements were carried out on measuring channel with L-fucosides at a flow rate of 5 μ l min⁻¹. Protein PHL at a concentration of 20 μ g mL⁻¹ was mixed with various concentrations of inhibitors (500 – 5 μ M) and injected onto the sensor chip. The response of lectin bound to the sugar surface at equilibrium was plotted against the concentration of inhibitor in order to determine IC₅₀ (concentration of inhibitor resulting in 50% inhibition of binding). As IC₅₀ is not a constant and depends on the experimental set-up, a parameter called potency was used for characterization. The potency of a tested inhibitor is the ratio of IC₅₀ of a chosen standard inhibitor (in this case L-fucose) and the inhibitor in question. Pure PHL lectin was used as a control (0% inhibition) and channel with pure biotin served as a blank.

Isothermal titration calorimetry

PHL protein in buffer A was equilibrated at room temperature at least for 30 min before ITC measurement. All ITC experiments were performed using ITC200 calorimeter (Malvern Instruments Ltd., UK) at 25 °C. Carbohydrate ligands were dissolved in the same buffer and used at different concentrations. Protein in the calorimeter cell (50 μ M) was titrated by consecutive additions (2 μ l) of the ligand (1.5 – 50 mM) in the syringe while stirring at 1000 rpm. Control experiments (injections of individual ligands into the buffer A) were performed, and heat responses were subtracted. Integrated heat effects were analyzed by nonlinear regression using a single-site binding model in Origin 7 software (Microcal Instruments).^[22] At least two independent titrations were carried out for each tested ligand.

Crystallization and data collection

PHL was concentrated to 12.5 mg mL⁻¹ using an ultrafiltration unit with a 10-kDa cut-off membrane (Vivaspin 20, Sartorius, Germany). The crystal preparation was described previously.^[5] The crystals were obtained under the following conditions: 4 μ l sitting drop, protein solution mixed with precipitant (3.7-4.0 M NaCl, 100 mM Hepes pH 7.5) in ratios 1:1, 3:5, 1:3 and 1:7. The drops were set against 0.5 mL of the same equilibration precipitant. To determine the PHL structure complexed with ligands, the crystals of PHL were soaked in a 1 mM solution of compounds 16, 18, 19, 20 for 45 minutes or 2.5 mM solution of compound 5 for 20 minutes, respectively. The crystals were cryo-protected using 40% PEG 400 and frozen in liquid nitrogen. The diffraction data of PHL complexed with saccharides were collected at the BESSY II electron storage ring (Berlin-Adlershof, Germany).^[23]

Structure determination

Images were processed using XDSAPP^[24] and converted to structure factors using the program package CCP4 v.6.5^[25], with 5% of the data reserved for R_{free} calculation. The structure of PHL complex was solved by molecular replacement with MOLREP^[26] using the monomeric coordinates of the ligand-free PHL structure (PDB ID: 5MXE). Refinement of the molecule was performed using REFMAC5^[27] alternated with manual model building in Coot v.0.8.^[28] Sugar-derived ligand coordinates were established using JLigand^[29] included in CCP4 program package. Ligand and other compounds that were present were placed manually using Coot. Water molecules were added by Coot and checked manually. The addition of alternative conformations, where necessary, resulted in final structure that was validated using the ADIT (<http://rcsb.org>) and MolProbity^[30] (<http://molprobity.biochem.duke.edu>)

validation servers and was deposited in the PDB as entry 6F5W. Molecular drawings were prepared using Pymol (Schrödinger, Inc., USA).

¹H STD NMR experiment

STD experiments were performed for samples dissolved in D₂O (PBS, pH = 7.5, T = 298 K) with molar ratio of ligand to PHL of about 100:1. Protein concentration was kept as low as ca. 10 μM to avoid aggregation of PHL upon adding ligands. A train of band-selective E-BURP-1 shaped pulses of 50 ms each with a maximum B1 field strength of 90 Hz was employed for selective saturation of protein magnetization in total of 3 s. An off-resonance frequency of δ = -27 ppm and on-resonance frequencies of δ = -1.5 ppm for irradiation at aliphatic signal region and of δ = 10.5 ppm for aromatic region of PHL were applied. Off- and on-resonance data were recorded at alternate scans and the corresponding FIDs were collected in separate memories for subsequent processing and for the generation of STD spectra. The STD intensities given in Figs. 6. and 7. were normalized with respect to that of H-1 proton (100 %) obtained upon irradiating at the aliphatic signal region of protein.

P. asymbiotica growth

P. asymbiotica subsp. *australis* was inoculated from a stock cells stored at -80 °C into a standard LB media and were grown in 30 °C under an orbital shaking overnight. Bacterial growth was tracked by measuring the optical density of the broth at 600 nm (OD₆₀₀) using a spectrophotometer (WPA CO8000 Biovawe Cell Density Meter, Biochrom Ltd., UK). Cells were harvested when reaching a OD₆₀₀ = 0.5. The culture was centrifuged at 4,300 g and 22 °C for 2 minutes (Eppendorf centrifuge MiniSpin, Eppendorf, Germany) and cells were then washed three times by PBS (137 mM NaCl, 2.7 mM KCl, 10 mM Na₂HPO₄, 1.8 mM KH₂PO₄). Cells were diluted in PBS to OD₆₀₀ of 2.0 and kept in a fridge until performing the aggregation assay.

Cell aggregation assay

Fucosylated compounds were diluted in dimethylsulfoxide (DMSO) to a final concentration of 50mM. *P. asymbiotica* subsp. *australis* cells and ligands were gently mixed in a 1:1 (v/v) ratio. Ligands were diluted to a final concentration ranging from 25 mM to 0.3125 mM. The reaction mixtures were left at room temperature for 30 min. 5 μl of reaction mixture were then transferred onto a microscope slides. As a negative control, bacterial cells were mixed with DMSO in absence of fucosylated inhibitors to a final concentration of DMSO of 50 % at an OD₆₀₀ of 1.0. Microscopic observation was performed at 200x magnification using an optical microscope (Olympus IX81 Microscope IX81F-3 with IX2-UCB-2 Controller and X-Cite 120PC Q; Olympus, Japan and Excelitas Technologies, USA).

Acknowledgements

The synthetic work was supported by National Research, Development and Innovation Office of Hungary (K119509, M. Csávás) and the EU and co-financed by the European Regional Development Fund under the project GINOP-2.3.2-15-2016-00008. The project was further supported by the János Bolyai Fellowship of the Hungarian Academy of Sciences (M. Csávás). The work covering structure and function studies was supported by the by Ministry of Education, Youth and Sports within

programme INTER COST (project No. LTC17076), and from European Regional Development Fund-Project „CIISB4HEALTH“ (No. CZ.02.1.01/0.0/0.0/16_013/0001776). CIISB research infrastructure project LM2015043 funded by MEYS CR is also gratefully acknowledged for the financial support of the measurements at the CF Biomolecular Interactions and Crystallization. CEITEC, Masaryk University, Brno, Czech Republic. Especially, we would like to thank Jitka Ždánková, Jan Komárek and Lenka Malinová for their help with lectin characterization. We also wish to thank the BESSY II electron storage ring (Berlin-Adlershof, Germany) for access to their synchrotron data collection facilities and allocation of synchrotron radiation beam time. The funders had no role in study design, data collection and analysis, decision to publish, or preparation of the manuscript. We also thank Ben Watson-Jones for language corrections.

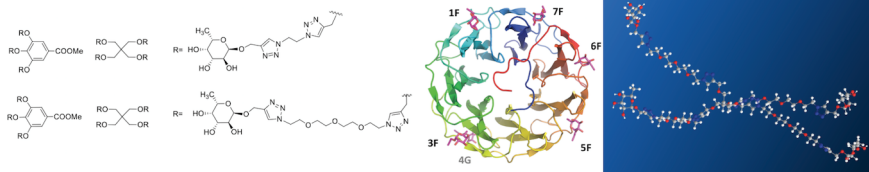
Keywords: fucoclusters • lectin • multivalency • *Photorhabdus asymbiotica* • agglutination

- [1] J. G. Gerrard, N. R. Waterfield, R. Vohra, R. French-Constant, *Microbes Infect.* **2004**, *6*, 229–237.
- [2] N. R. Waterfield, T. Ciche, D. Clarke, *Annu. Rev. Microbiol.* **2009**, *63*, 557–574.
- [3] S. C. P. Costa, P. A. Girard, M. Brehélin, R. Zumbihl, *Infect. Immun.* **2009**, *77*, 1022–1030.
- [4] J. G. Gerrard, N. R. Waterfield, M. Sanchez-Contreras, *Clin. Microbiol. Newsl.* **2011**, *33*, 103–109.
- [5] G. Jančaříková, J. Houser, P. Dobeš, G. Demo, P. Hyřil, M. Wimmerová, *PLOS Pathog.* **2017**, *13*, e1006564.
- [6] M. Csávás, L. Malinová, F. Perret, M. Gyurkó, Z. T. Illyés, M. Wimmerová, A. Borbás, *Carbohydr. Res.* **2017**, *437*, 1–8.
- [7] M. Herczeg, E. Mező, N. Molnár, S.-K. Ng, Y.-C. Lee, M. Dah-Tsy Chang, A. Borbás, *Chem. Asian J.* **2016**, *11*, 3398–3413.
- [8] J. Camponovo, J. Ruiz, E. Cloutet, D. Astruc, *Chem. Eur. J.* **2009**, *15*, 2990–3002.
- [9] P. Xu, R. Castelli, P. Kováč in P. Kováč, G. van der Marel, J. Codée (Eds.), *Carbohydrate Chemistry: Proven Synthetic Methods*, CRC Press, Boca Raton, **2014**, Vol 2. pp. 213–216.
- [10] D. J. Leaver, R. M. Dawson, J. M. White, A. Polyzos, A. B. Hughes, *Org. Biomol. Chem.* **2011**, *9*, 8465–8474.
- [11] A. Nadler, C. Hain, U. Diederichsen, *Eur. J. Org. Chem.* **2009**, *2009*, 4593–4599.
- [12] G. Guchhait, A. K. Misra, *Catal. Commun.* **2011**, *14*, 52–57.
- [13] M. Abellán Flos, M. I. García Moreno, C. Ortiz Mellet, J. M. García Fernández, J.-F. Nierengarten, S. P. Vincent, *Chem. - Eur. J.* **2016**, *22*, 11450–11460.
- [14] L. N. Goswami, Z. H. Houston, S. J. Sarma, S. S. Jalisatgi, M. F. Hawthorne, *Org. Biomol. Chem.* **2013**, *11*, 1116–1126.
- [15] M. Mayer, B. Meyer, *Angew. Chem. Int. Ed.* **1999**, *38*, 1784–1788.
- [16] M. Mayer, B. Meyer, *J. Am. Chem. Soc.* **2001**, *123*, 6108–6117.
- [17] P. Groves, K. E. Kövér, S. André, J. Bandorowicz-Pikula, G. Batta, M. Bruix, R. Buchet, A. Canales, F. J. Cañada, H.-J. Gabius, et al., *Magn. Reson. Chem.* **2007**, *45*, 745–748.
- [18] A. M. Boukerb, A. Rousset, N. Galanos, J.-B. Méar, M. Thépaut, T. Grandjean, E. Gillon, S. Cecioni, C. Abderrahmen, K. Faure, et al., *J. Med. Chem.* **2014**, *57*, 10275–10289.
- [19] G. Yu, Y. Ma, C. Han, Y. Yao, G. Tang, Z. Mao, C. Gao, F. Huang, *J. Am. Chem. Soc.* **2013**, *135*, 10310–10313.
- [20] J. E. Gestwicki, L. E. Strong, C. W. Cairo, F. J. Boehm, L. L. Kiessling, *Chem. Biol.* **2002**, *9*, 163–169.
- [21] L. Adamová, L. Malinová, M. Wimmerová, *Microsc. Res. Tech.* **2014**, *77*, 841–849.
- [22] T. Wiseman, S. Williston, J. F. Brandts, L.-N. Lin, *Anal. Biochem.* **1989**, *179*, 131–137.
- [23] U. Mueller, N. Darowski, M. R. Fuchs, R. Förster, M. Hellmig, K. S. Paithankar, S. Pühringer, M. Steffien, G. Zocher, M. S. Weiss, *J. Synchrotron Radiat.* **2012**, *19*, 442–449.

- [24] M. Krug, M. S. Weiss, U. Heinemann, U. Mueller, *J. Appl. Crystallogr.* **2012**, *45*, 568–572.
- [25] M. D. Winn, C. C. Ballard, K. D. Cowtan, E. J. Dodson, P. Emsley, P. R. Evans, R. M. Keegan, E. B. Krissinel, A. G. W. Leslie, A. McCoy, et al., *Acta Crystallogr. D Biol. Crystallogr.* **2011**, *67*, 235–242.
- [26] A. Vagin, A. Teplyakov, *Acta Crystallogr. D Biol. Crystallogr.* **2010**, *66*, 22–25.
- [27] G. N. Murshudov, P. Skubák, A. A. Lebedev, N. S. Pannu, R. A. Steiner, R. A. Nicholls, M. D. Winn, F. Long, A. A. Vagin, *Acta Crystallogr. D Biol. Crystallogr.* **2011**, *67*, 355–367.
- [28] P. Emsley, B. Lohkamp, W. G. Scott, K. Cowtan, *Acta Crystallogr. D Biol. Crystallogr.* **2010**, *66*, 486–501.
- [29] A. A. Lebedev, P. Young, M. N. Isupov, O. V. Moroz, A. A. Vagin, G. N. Murshudov, *Acta Crystallogr. D Biol. Crystallogr.* **2012**, *68*, 431–440.
- [30] V. B. Chen, W. B. Arendall, J. J. Headd, D. A. Keedy, R. M. Immormino, G. J. Kapral, L. W. Murray, J. S. Richardson, D. C. Richardson, *Acta Crystallogr. D Biol. Crystallogr.* **2010**, *66*, 12–21.

Entry for the Table of Contents

FULL PAPER



Gita Jančaříková, Mihály Herczeg, Eva Fujdiarová, Josef Houser, Katalin E. Kövér, Anikó Borbás,* Michaela Wimmerová* and Magdolna Csávás*

Page No. – Page No.

Synthesis of α -L-fucopyranoside-presenting glycoclusters and investigation of their interaction with *Photorhabdus asymbiotica* lectin (PHL)

A novel class of α -L-fucopyranoside-presenting glycoclusters have been synthesized to target multiple binding sites of PHL lectin from *Photorhabdus asymbiotica*. The interaction between fucosides and PHL was investigated by biological methods, X-ray crystallography and STD-NMR. The potency of ligands depended on their valency and architecture, but all fucoclusters proved to be up to several orders of magnitude better ligands than its natural ligand, L-fucose.

Accepted Manuscript